CELL NUCLEI DETECTION AND SEGMENTATION FOR COMPUTATIONAL PATHOLOGY USING DEEP LEARNING

Kemeng Chen
Ning Zhang

Department of Electrical and Computer Engineering

The University of Arizona,1230 E. Speedway, Blvd, Tucson, AZ, USA
{kemengchen, zhangning}@email.arizona.edu

Linda Powers
Janet Roveda

Department of Electrical and Computer Engineering, Biomedical Engineering, BIO5 Institute
The University of Arizona, 1230 E. Speedway, Blvd, Tucson, AZ, USA
{lspowers, meilingw}@email.arizona.edu

ABSTRACT

This work presents a deep learning model and image processing based processing flow to detect and segment nuclei from microscopy images. This work aims at isolating each nuclei by segmenting the boundary and detecting the geometric center of the nuclei. The deep learning model employs a multi-layer convolutional neural network based architecture to extract features from both spatial and color information and to generate a gray scaled image mask. Subsequent image processing steps smooth nuclei boundaries, isolate each individual nuclei and calculate the geometric center of the nuclei. The proposed work has been implemented and tested using H&E stained microscopy images containing seven different tissue samples. Experimental results demonstrated an average precision of 0.799, recall of 0.955, F-score of 0.86, and IoU of 0.835.

Keywords: Nuclei, detection, segmentation, deep learning, image processing

1 INTRODUCTION

The detection and segmentation of nuclei constitutes an important step in pathology based diagnoses, such as cancer diagnosis, grading and quantitatively analysis, which influence decision reliability (Irshad et al. 2014). However, manual segmentation is intensive and time consuming work for pathologists. Thus, computer based methods have been introduced to automate this process. However, automated nuclei detection and segmentation is faced with multiple challenges. For example, nuclei exhibit different morphologies that may depend on the cell type, disease state, cell life cycle, etc., and exist in backgrounds of various tissue morphologies which make it difficult to detect and segment them (Irshad et al. 2014). In addition, nuclei often exist close to each other which pose a challenge for their separation (Irshad et al. 2014; Kumar et al. 2017).

Thus, this work implements a deep learning based processing flow incorporating image processing to detect and segment nuclei from microscopic images. The model separates closely spaced nuclei by using a customized loss function which puts more emphasis on adjacent edges during the training process. The processing flow in this work also adopts morphological operations to assist locating the geometric center of each nuclei and isolate each individual nuclei.

The rest of the paper is organized as the following: section 2 is a brief review of related works in the literature. Section 3 introduces the deep learning model and image processing in detail. Section 4 shows our results using H&E stained images. Finally, the paper concludes in section 5.

SpringSim-MSM, 2019 April 29-May 2, Tucson, AZ, USA;

2 LITERATURE REVIEW

Methods used in automated nuclei segmentation and detection works in the literature ranged from threshold, and morphological segmentation to machine learning. For example, Otsu algorithm (Otsu 1979) calculated an optimal threshold value such that background and foreground's variance are minimalized. After segmentation, nearby objects can be separated by morphological operations such as watershed algorithm. In recent years, machine/deep learning based methods are widely adopted in computational pathology. Deep learning models such as image to pixel architecture (Kuma et al. 2017) usually uses 2D convolutional neural network followed by a fully connected neural network. This kind of model takes an image patch and output one pixel in the mask. In contrast, image to mask models (Olaf et al. 2015) maps an image or patch directly to mask of the same size. The model proposed in this work contains both an image patch-to-patch model and image processing based flow. By adopting overlapping patch strategy, each pixel in the output mask is determined by multiple patches and thus enhance robustness.

3 METHOD

Our method first utilized the feature learning capability of deep learning (LeCun et al. 2015) to estimate the probability of each pixel to be a cell nuclei and then used image processing to smooth the boundary and detect each individual nuclei. Figure 1 shows the block diagram of the processing flow. Our model first partitions tissue images into overlapping patches as the model input. Our model is based on the U-net model. The U-Net model (Olaf et al. 2015) is a multi-layer convolutional neural network which integrates down sampling and up sampling on the input image in the spatial direction (height and width) between successive convolutional layers. Thus, down sampling and up sampling makes the architecture symmetric as shown in Figure 1 (U-Net Model).

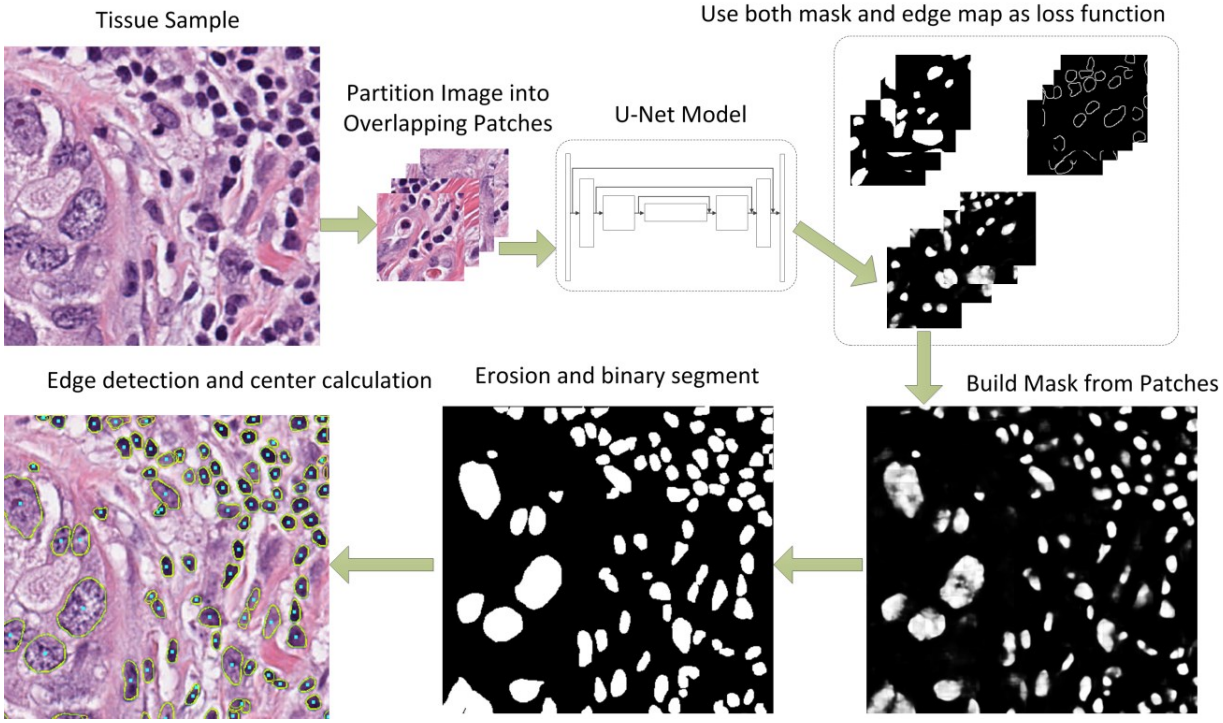

Figure 1. Block diagram of the proposed deep learning based nuclei segmentation and detection processing flow.

In addition, the U-net model contains the contracting path to propagate the image to layers of the same size (Olaf et al. 2015). This architecture explores the sparsity of natural images and is proven to achieve good performance in biomedical image segmentation tasks. To enhance separation ability of nearby nuclei, our model used both a ground truth mask and edge map (calculated from ground truth mask) in the loss function during the training. Output of our model are gray scaled mask patches.

Mask of the entire image is then recovered by averaging overlapping patches. As we adopted the overlapping patch strategy, the value of each pixel in the mask is determined by multiple patches which enhance performance robustness. To smooth the segmented boundary, we applied erosion operations on mask and isolate each enclosing ellipse as each individual nuclei. Finally, we calculate and label the geometric center of each nuclei to count the number of nuclei.

To enhance the edge separation, we designed the loss function in the training as a combination of both mask difference and edge difference. We defined the ground truth mask $\hat{y}_i$ *(i∈K)* and our model's output as y_i *(i∈K)*. We also defined $\hat{e}_j$ *(j∈S)* as the edge map of $\hat{y}_i$ and e_j *(j∈S)* as the edge map for y_i. Our loss function is the weighted sum of both edge loss and mask loss as shown in (1).

$$Loss = w \cdot \sum_{i \in K} (\hat{y}_i - y_i) + (1 - w) \cdot \sum_{j \in S} (\hat{e}_j - e_j) \ . \tag{1}$$

4 EXPERIMENTAL RESULTS

To validate the proposed method, we implemented the proposed work using Python 3.4 with TensorFlow 1.3 and OpenCV and tested our model with H&E stained images containing multiple types of tissues (Kumar et al. 2017). Specific implementation of our model is listed in Table 1. Our model input is a three channel RGB image patch of size 128x128x3. Within our model, the patch size is first changed to 16x16x32 and then back to 128x128x1 (one channel mask). The first column is the contract we selected to forward image to the corresponding layer of the same size. For example, layer 2 not only passes its information to layer 3 but also to layer 6, which receives information from both layer 5 and layer 2. Layer 6 first concatenates that information and then process it. We use the ReLu function across each layer and a filter of size 3x3 is selected to achieve the best performance (discussed later in this section).

Table 1. Deep learning model configurations and parameters.

Contract path	Image size	Filter size	# of filters	Sampling	Activation
(1) to (2, 7)	128x128x3	3x3x3	8	Down sample	ReLu
(2) to (3, 6)	64x64x8	3x3x8	16	Down sample	ReLu
(3) to (4, 5)	32x32x16	3x3x16	32	Down sample	ReLu
(4) to (5)	16x16x32	3x3x32	16	N/A	ReLu
(5) from (3, 4)	32x32x(16+16)	3x3x32	8	Up sample	ReLu
(6) from (2, 5)	64x64x(8+8)	3x3x16	3	Up sample	ReLu
(7) from (1, 6)	128x128x(3+3)	3x3x6	1	N/A	ReLu
Output	128x128x1	N/A	N/A	N/A	N/A

To quantitatively measure the performance of our model, we introduced four metrics: precision, recall, and F-score as defined in (2) (3) and (4) where TP is true positive, FP is false positive, and FN is false negative. In our evaluation metrics, we defined TP as when our model successfully detects nuclei. FP is

defined when our model detects a nuclei which is actually background. FN is defined when a true nuclei is not detected by our model. Precision, recall, and F-score measures the performance of nuclei detection.

$$precision = \frac{TP}{TP + FP} , \tag{2}$$

$$recall = \frac{TP}{TP + FN} , \tag{3}$$

$$Fscore = 2 \times \frac{precision \times recall}{precision + recall} . \tag{4}$$

To measure the performance of segmentation, we adopt intersection over union (IoU). IoU measures the intersection over union of nuclei areas on a ground truth mask and our model result as the A and B in (5).

$$IoU(A, B) = \frac{A \cap B}{A \cup B} . \tag{5}$$

Preliminary results tested on 30 H&E stained images of size 1000x1000 show that the proposed model achieves a recall of 0.955, precision of 0.799, F-Score of 0.87, and mask Intersection over Union (IoU) of 0.835.

Figure 2 shows the visual results of nuclei boundary segmentation and geometric center detection. Light blue dots represent the center of each nucleus identified by our model and the boundary contour is marked in green. Yellow lines are the original ground truth masks of each nucleus. We show our result on seven different tissues which have different colors, background texture, nuclei shape, and size.

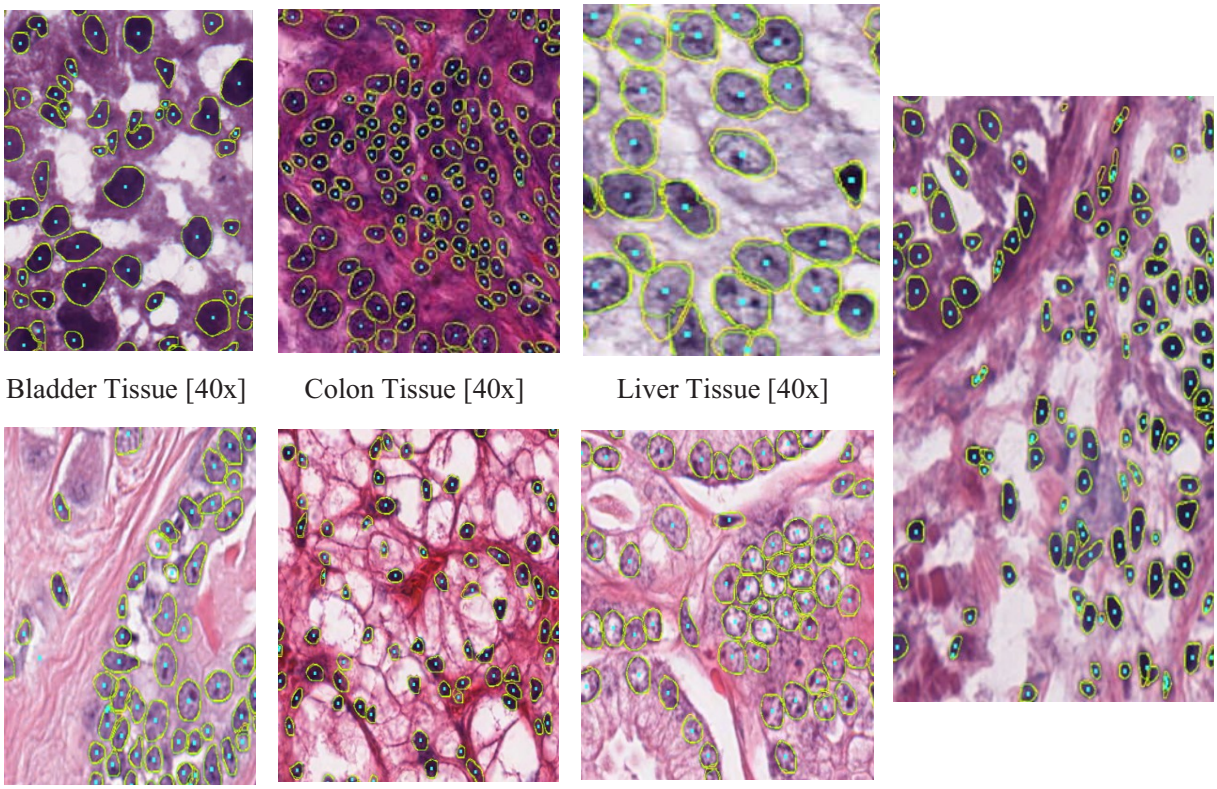

Bladder Tissue [40x] Colon Tissue [40x] Liver Tissue [40x]

Breast Tissue [40x] Kidney Tissue [40x] Prostate Tissue [40x] Stomach Tissue [40x]

Figure 2. Nuclei segmentation and detection on seven different kinds of tissues.

The convolutional neural network mimics the process of filtering and learns filter coefficients from the data. Thus filter shape and size have an strong influence on the feature learning capability and thus segmentation result. To study the effect of filter size and shape in our convolutional neural network model, we tested different filter shapes using heights and widths from 2 to 7. The IoU results are shown in Table 2. The first column is the size of filter height and first row is the filter width. Based on result in Table 2, we selected a filter size of 3x3 for our model as shown in Table 1 as it achieves the highest IoU among our experiments. Table 3 is a comparison of the proposed work with relevant works in the literature. We compared works target on nuclei detection and segmentation tasks in terms of F-score.

Table 2. IoU from using filters of different shape, size in convolutional neural network.

Filter size	2	3	4	5	6	7
2	0.796	0.819	0.812	0.808	0.787	0.770
3	0.820	0.835	0.819	0.808	0.783	0.762
4	0.814	0.821	0.802	0.787	0.762	0.740
5	0.809	0.808	0.786	0.767	0.742	0.719
6	0.788	0.783	0.760	0.741	0.716	0.695
7	0.769	0.761	0.735	0.735	0.693	0.672

Table 3. Comparison with other related works in the literature.

	Method	Task	precision	recall	F-score
Proposed work	U-Net, image processing	Pathology	0.799	0.955	0.860
Kuma et al.	Deep learning	Pathology	NA	NA	0.826
Khan et al.	Sparse Representation	Histology	0.849	0.872	0.861

5 CONCLUSION AND OUTLOOK

This work proposed and implemented a deep learning and image processing based strategy for cell nuclei detection and segmentation. Experimental results tested on seven tissues show an averaged precision of 0.799, recall of 0.955, F score of 0.87 and IoU of 0.835. In the future, the model could be further improved to overcome overlapping nuclei by a second detection based on nuclei centers.

REFERENCES

Irshad, H., A. Veillard, L. Roux, and D. Racoceanu, 2014, "Methods for Nuclei Detection, Segmentation, and classification in Digital Histopathology: A Review – Current Status and Future Potential", *IEEE Reviews in Biomedical Engineering*, vol. 7, pp. 97-114.

Kumar, N., R. Verma, S. Sharma, S. Bhargava, A. Vahadane, and A. Sethi, 2017, "A Dataset and a Technique for Generalized Nuclear Segmentation for Computational Pathology", *IEEE Transactions on Medical Imaging*, vol. 36, pp. 1550-1560.

LeCun, Y., Y. Bengio, and G. Hinton, 2015, "Deep Learning", *Nature*, vol. 521, pp. 436-444.

Otsu, N., 1979, "A Threshold Selection Method from Gray-Level Histograms", *IEEE Transactions on systems, man, and cybernetics*, vol. 9, pp. 62-66.

Ronneberger, o., P. Fischer, T., Brox, 2015, "U-Net: Convolutional Networks for Biomedical Image Segmentation", *International Conference on Medical Image Computing and computer-assisted intervention, Spring, Cham*, pp. 234-241.

Sirinukunwattana, K., A. M. Khan, and N. M. Rajpoot, 2015, "Cell words: modelling the visual appearance of cells in histopathology images," *Computerized Medical Imaging and Graph*, vol. 42, pp. 16–24.

AUTHOR BIOGRAPHIES

KEMENG CHEN received his B.S. degree in Electrical and Information Engineering from Tianjin Polytechnic University. He is currently pursuing his Ph.D. degree in Electrical and Computer Engineering at the University of Arizona. His email address is kemengchen@email.arizona.edu.

NING ZHANG received his B.S. degree in Electrical and Computer Engineering at the University of Arizona in 2018. He is current pursuing his Ph.D. degree in Management of Information System at The University of Arizona. His email address is zhangning@email.arizona.edu.

PROFESSOR DR. LINDA S. POWERS is the Thomas R. Brown Chair in Bioengineering, Professor of Electrical and Computer Engineering and Professor of Biomedical Engineering at the University of Arizona. Before joining the University of Arizona faculty, she was a member of the technical staff of AT&T Bell Laboratories [1976-1988], an Adjunct Professor of Biochemistry and Biophysics at the University of Pennsylvania [1978-1998], and Professor of Electrical and Computer Engineering at Utah State University [1998-2006]. She is a fellow of the American Physical Society and the American Institute of Chemists and her honors include the First US Bioenergetics Award of the Biophysical Society. Professor Powers earned her B.S. in physics and also in chemistry at Virginia Polytechnic Institute and State University and her M.A. in physics and Ph.D. in biophysics at Harvard University. Her current research efforts involve the detection and identification of microbial (bacteria, viruses, fungi, toxins) contamination with applications to foods/water/air quality, sterilization/decontamination, medical diagnostics, homeland security, and the search for life in extreme environments as surrogates for the moon, Mars, and Europa.. Her email address is lspowers@email.arizona.edu.

PROFESSOR DR. JANET ROVEDA is a Professor in the Department of Electrical and Computer Engineering at the University of Arizona in Tucson. She received her M.S. and Ph.D. degrees in Electrical Engineering and Computer Sciences from the University of California, Berkeley in 1998 and 2000, respectively. She was a recipient of the NSF career award and the Presidential Early Achievement Award for Science and Engineering at White House in 2005 and 2006, respectively. She was the recipient of the 2008 R. Newton Graduate Research Award from the EDA community, and the 2007 USS University of Arizona Outstanding Achievement Award. She received the best paper award in journal of clean energy in 2013, ISQED 2010 as well as best paper nominations in ASPDAC 2010, ICCAD 2007, and ISQED 2005. Her primary research interests focus on robust VLSI circuit design, biomedical instrumentation design, Smart grid, VLSI circuit modeling/design and analysis, and low power multi-core system design. She has over 120 publications.. Her email address is meilingw@email.arizona.edu.